ACERP: Vol. 4, No. 3 & 4, (Summer & Fall 2018) 8-15

Advanced Ceramics Progress

Research Article

Journal Homepage: www.acerp.ir

Evaluation of mechanical properties and apatite formation of synthesized fluorapatite-hardystonite nanocomposite scaffolds

E. Abdolahi and H. R. Bakhsheshi-Rad*

Advanced Materials Research Center, Department of Materials Engineering, Najafabad Branch, Islamic Azad University, Najafabad, Iran

PAPER INFO

Paper history:

Received 31 March 2019
Accepted in revised form 23 April 2019

Keywords:

Fluorapatite
Hardystonite
Scaffold
Bone tissue engineering scaffold

ABSTRACT

In this study, mechanical properties and apatite formation ability of synthesized fluorapatite-hardystonite (FA-HT) nanocomposite scaffolds were investigated. Hardystonite (HT; 5 and 10 wt.%) as a reinforcement phase was incorporated into the FA scaffold. FA was mixed with HT for 4 h under argon gas at 220 °C. A space holder method was used for fabricating porous FA-HT scaffolds. Sodium chloride (NaCl) was used as pore-forming agent in this method. Then, the powder was compacted under a pressure of 220 MPa. Finally, the samples were sintered at 1000 ºC for 2 h. The X-ray diffraction (XRD) results of the synthesized scaffolds confirmed the formation of FA and HT powders. Studying the microstructure of the samples showed that synthesized scaffolds had a porous structure with interconnected pores, similar to the porosity degree of natural bones. The results also revealed that the mechanical properties of scaffolds were improved; the compressive strength values of the FA-5HT and FA-HT scaffolds were obtained 1.6 MPa and 2.8 MPa, respectively. The young modulus values for these scaffolds were 5.5 MPa and 12.4 MPa, respectively. Results of bioactivity test showed the ratio of calcium to phosphate (Ca/P) in scaffolds was 1.71±0.3 and 1.60±0.5 for FA-5HT and FA-10HT samples, respectively. Based on the results, FA-HT scaffolds have desirable mechanical properties and suitable level of bioactivity which can be used as new and promising biomaterials in bone tissue engineering and repairing bone defects.

1. INTRODUCTION

Bone defects are among the greatest challenges in medical science. These defects happen in different forms and cost a huge amount of money to be treated every year [1–3]. Bone fractures caused by osteoporosis and bone defects that happen during chemotherapy are among the examples of bone defects [4]. The healing process of bones faces serious problems when pathologic fractures happen and/or when bones are seriously damaged [5]. Tissue engineering is a new and growing method which has attracted attentions these days [5]. Tissue engineering is being used for repairing tissues such as bones, cartilages, blood vessels, and skin. In tissue engineering applications, cells are cultured on scaffolds that are developed from natural polymers [3,6]. Biomaterials used as scaffolds in bone tissue engineering must be highly biocompatible and have a proper level of biodegradability. Nowadays, compositions of different particles are used in order to control the degradability and mechanical properties in different types of scaffolds [3,6,7]. Some other important factors in designing scaffolds are controlling the shape, size, distribution, interconnectivity of pores, and maintaining the required thickness and strength necessary for transplant surgery [8]. Calcium phosphate (Ca-P)-based and calcium silicate-based bio-ceramics are suitable options for this purpose, due to their appropriate mechanical properties, biocompatibility and bioactivity [9–11]. Bio-ceramic scaffolds have attracted attentions of biomedical engineers because of their satisfactory mechanical properties, biocompatibility and bioactivity. So, they seem to be suitable for designing and fabricating bone tissue scaffolds [12]. Fluorapatite ($Ca_5(PO_4)_3F$), as a Ca-P ceramic is widely used in bone tissue engineering because of its good biodegradation, biocompatibility,

* *Corresponding Author Email: rezabakhsheshi@pmt.iaun.ac.ir; rezabakhsheshi@gmail.com (R. Bakhsheshi-Rad)*

adsorption properties which helps growth and adhesion of cells in culture medium, porous structure, and apatite-forming ability [2,3]. Despite its perfect biological properties, fluorapatite has poor mechanical properties that limit its application in load bearing when transplanting inside the body. As a result, adding a second phase to the based scaffold in order to increase its strength can be a good method for improving the mechanical integrity of the scaffold. Hence, in this study, hardystonite (Ca_2ZnSi_2O) as a Ca-containing silicate ceramics was used as the second phase for improving the compressive strength of the scaffolds [3,13]. In another study [6] it was shown that the presence of zinc in the hardystonite had a physiologic effect on the growth and mineralization of bone tissue. As people get older, the amount of zinc element (in their body) decreases and as a result, bone load will decrease. Likewise other studies [7] exhibited that bio-ceramic containing zinc, such as hardystonite can stimulate the activity of osteoblasts and facilitate bone formation. In addition to improving bioactivity, zinc can enhance mechanical properties such as compressive strength of scaffolds [14]. Zinc has also shown antibacterial properties. In this regard, hardystonite recently attracted great attentions due to its high bioactivity and biocompatibility and also having better mechanical properties than fluorapatite [6,7,9]. This bio-ceramic has a tetragonal structure with high flexural strength (131 MPa), good fracture toughness (1/2 $MPa \cdot m^{1/2}$), and suitable Young's modulus (33 GPa) [10]. Many studies have shown an excellent bone formation ability for composites containing hardystonite [7,15,16]. Space holder method is a viable method for fabrication of metallic and ceramic-based scaffolds. In this method, temporary powder particles, known as space holders, are designed to be a single structure for the scaffold. Generally speaking, space holder scaffold fabrication technique can be divided into four steps: 1) mixing the ceramic base powder with the space holder particles, 2) compacting these powders, 3) eliminating space holder particles by increasing the temperature, and 4) sintering the porous scaffold's precursor [7,17]. This method is easy and affordable and the resulting scaffolds have a porous structure, high mechanical strength and high specific surface areas which make them good hosts for adhesion, growth and proliferation of cells. To the best of our knowledge, this is the first report of the fabrication and characterization of an FA-HT scaffold targeting bone regeneration that demonstrates mechanical and bioactivity characteristic.

However, less information is available on the effects of the HT reinforcement phase to FA-based scaffolds and also its mechanical properties and bioactivity. Therefore, the main purpose of this project was preparation of FA-HT nanocomposite scaffolds with different concentration of HT by the space holder method in order to achieve desired mechanical properties along with the biological activity. Subsequently, the mechanical properties and the apatite-forming ability in the surface of the scaffolds in simulated body fluid (SBF) solution were investigated.

2. EXPERIMENTAL PROCEDURES

Fluoride powder (CaF_2, Sigma Aldrich, Germany, 99.99% purity), phosphorus pentoxide powder (P_2O_5, Merck, 98% purity, particle size <10 μm), calcium hydroxide powder ($Ca(OH)_2$, Merck, 99%purity), zinc oxide powder (ZnO, Merck, 99.5% purity, particle size < 0.8 μm), calcium carbonate powder ($CaCO_3$, Merck, 99.98% purity, particle size <13 μm) and sodium chloride powder (NaCl, Fluka, 99.9% purity, particle size <500μm) were used as starting materials. For preparation of FA-HT scaffolds, FA was mixed with different percentages of HT (5 and 10 wt. %) for 4 h under argon gas at 220 °C. Then space holder method was used for fabricating porous FA-HT scaffolds and sodium chloride (NaCl) with particle size of 400 to 600 μm was used as pore forming agent. Subsequently, the powders were compacted under 220 MPa at a speed of 2 mm/min. Then, the samples were kept at 180°C for 2h in order to remove the NaCl particles and obtain a scaffold with porous structure. Finally, the samples were sintered at 1000 ºC for 2h. Fig. 1. Shows the prepared fluorapatite containing 10 wt. % hardystonite (FA-10 %wt. HT) scaffolds before and after the sintering process. Microstructures of the FA-HT scaffolds were studied using transmission electron microscopy (TEM, Hitachi HT7700, Japan) and scanning electron microscopy (SEM, JEOL JSM-6380LA, Japan) equipped with energy dispersive X-ray spectroscopy (EDS; JEOL Inc., Tokyo, Japan). To measure the FA-HT scaffold pores size, the Image J software (version 1.47) was used. An X-ray diffractometer (Siemens D5000) was used to determine the phase components using Cu-Kα radiation (45 kV, 40 mA) over diffraction angles (2θ) of 20–65° at a scanning speed of 2°/min. All of the FA-HT scaffolds were tested by Fourier-Transform Infrared Spectroscopy (FTIR; Spectrum RXI, Perkin Elmer, USA) in order to identify and distinguish the functional groups in each sample. The FT-IR spectra were recorded in a spectral range of 4000–450 cm^{-1}. To study the bioactivity behavior, each of the FA-HT scaffolds was soaked in 100 mL of simulated body fluid (SBF) at 36.5 ± 1 °C for 28 d. The composition of the SBF solution was described in detail elsewhere [18]. After this time, the scaffolds were removed from the SBF cups and rinsed with distilled water and dried in the open air. In order to measure the compressive strength of the FA-HT scaffold with various amounts of HT, cylindrical specimens with the size of 8 mm (diameter) × 6 mm (height) were prepared according to ASTM E9 standard method. Subsequently, compression test was conducted using a Universal Testing Machine (Instron-5569) at a displacement rate of 0.5 mm/min at room temperature.

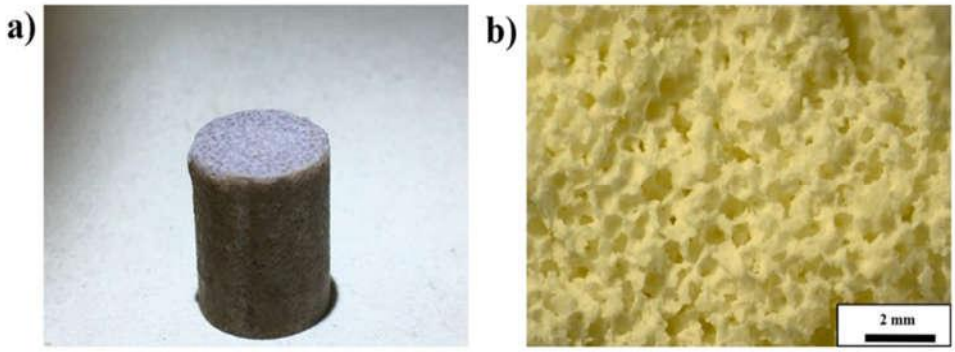

Figure 1. (a) Camera image of fabricated scaffolds before sintering and (b) Optical microscopy image of the scaffolds after sintering and removing NaCl particles

3. RESULTS AND DISCUSSION

3.1. Microstructure and composition

Fig. 2 shows SEM image of synthesized FA-xHT scaffolds (x=5 and 10 wt. %). As can be seen, the scaffolds had porous structures with interconnected pores. Porosity range was 500-600 µm for each scaffold. The average porosity of the samples was about 575 µm. Porosity percentage was calculated 67± 2% by Image J software. Previous studies [1,10] showed that an ideal scaffold for bone tissue engineering must have a porous structure with interconnected pores which let the oxygen and nutrients be exchanged and provide a suitable environment for cells to live, grow and migrate. Cells are not able to grow and reach the depth of scaffold in a non-porous structure and as a result, body rejects the scaffold after transplantation. Hence, the degree of porosity is one of the most important factors in designing a bone tissue engineering scaffold. Other studies revealed [11] that pore size plays an important role in cells' activity and optimum pore size for bone tissues is in the range of 550 µm and more. Pores in this range size can improve cell's migration, growth and proliferation. However, pores smaller than 300 µm are suitable for angiogenesis for nutrition exchanging of cells [19]. Size and percentage of pores can also affect the mechanical properties of the scaffold. Mechanical strength decreases as the size and percentage of pores increase. So these two parameters must be kept in an optimum state.

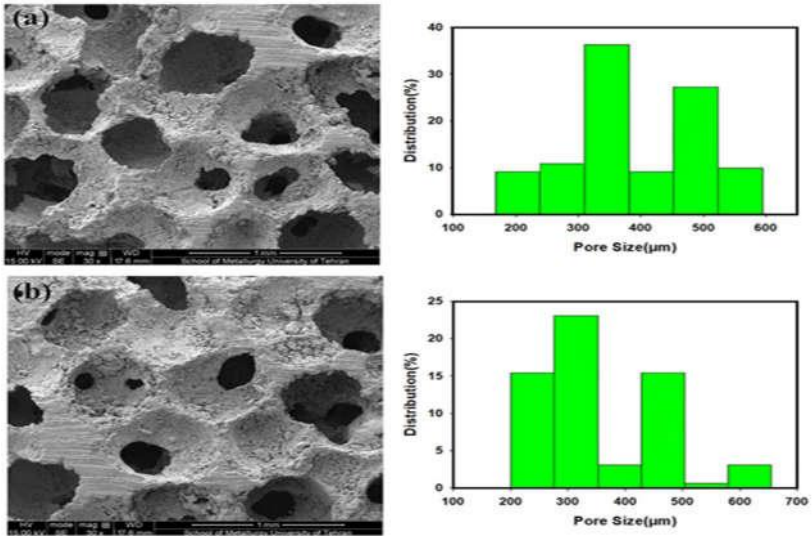

Figure 2. SEM images of FA-HT scaffolds with HT concentration of a) 5 and b) 10 wt.% and corresponding histogram image

Fig. 3 shows TEM images of fluorapatite and hardystonite synthesized powders. As can be seen, the morphology of mechanically alloyed synthesized powders was spherical and the diameter of particles was less than 100 nm. Nanostructure of these powders revealed their high reactivity, resulting from their high specific surface area (total surface area per volume). The high reactivity has a significant effect on biologic responses including mechanical and bioactivity properties. Nanostructured materials are more bioactive and shows higher apatite formation ability in comparison to macro-structured materials [20–22]. The TEM image also shows that nano-powders were agglomerated and adhered to each other which are signs of the high reactivity of synthesized nano-powders [23].

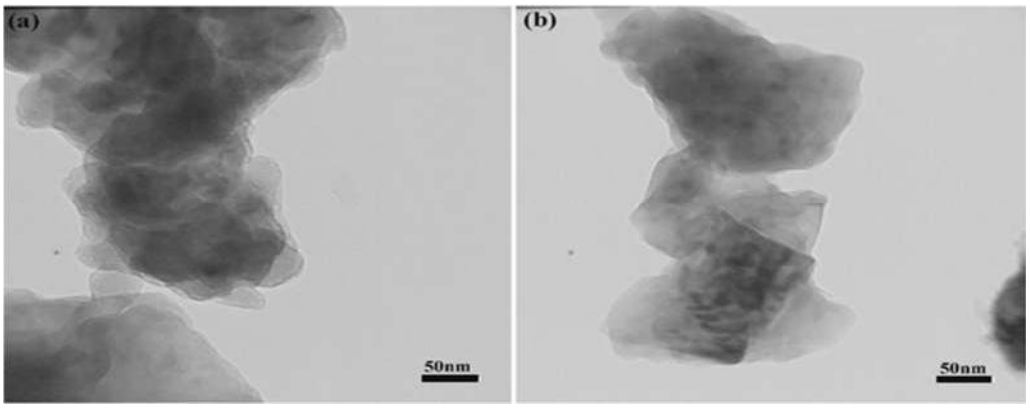

Figure 3. TEM images of a) fluorapatite and b) hardystonite powders

Fig. 4 shows the FTIR spectra of the FA-HT scaffolds with various HT concentrations. Peaks appeared at 573, 1037 and 1087 cm^{-1} are related to phosphate groups in fluorapatite [24]. While, The peaks at 617 and 1442 cm^{-1} can be ascribed to Si-O stretching vibration modes which indicates the formation of hardystonite [25]. The peak that has appeared at 499 cm^{-1} indicates the O-Ca-O bent bond in hardystonite [26,27]. The peak at 3450 cm^{-1} is due to the free O-H stretching. Asymmetric and symmetric stretching vibrations of P-O, appeared in peaks at 1037 and 1087 cm^{-1}, respectively.

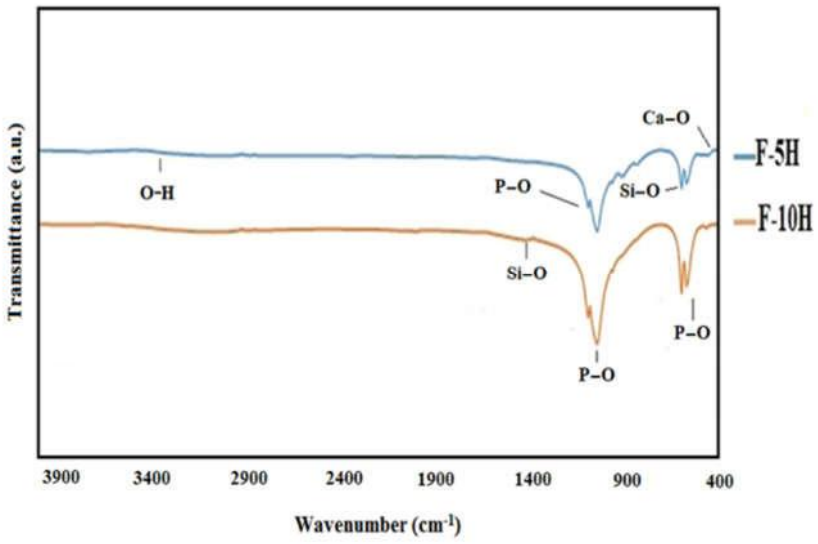

Figure 4. FT-IR absorption spectra of FA-HT scaffolds with various HT concentrations

Fig. 5 shows the XRD patterns of FA and HT powders as well as FA-HT scaffolds with various HT concentrations. As can be seen, XRD pattern of FA samples was related to fluorapatite phase ($Ca_5P_3FO_{12}$) with hexagonal crystal structure and had no extra peak, implying that there was no impurity in the synthesized powder. It should be noted that the XRD pattern of this phase matches the reference card number 01-071-0880. Similarly, the XRD pattern of the synthesized hardystonite powder through the sol-gel method showed the absence of impurity in the final products (JCPDS File No. 01-084-1319). It is worth mentioning that hardystonite has a tetragonal structure. It was also observed that after mixing the FA and HT powers for a long time via mechanical milling process, crystallites size decreased as the diffraction peaks become wider. Furthermore, the average crystallite size of the fluorapatite and hardystonite nano-powders obtained by the Williamson–Hall equation was about 88 ± 4 nm and 81 ± 4 nm, respectively. The characteristic peaks of HT and FA were detected with small peaks of SiO_2. No reaction occurred between the spacer and the mixed powders. Moreover, no sign of spacer agent (NaCl) was detected due to increasing a sintering temperature to 1250 °C to complete removing of the spacer.

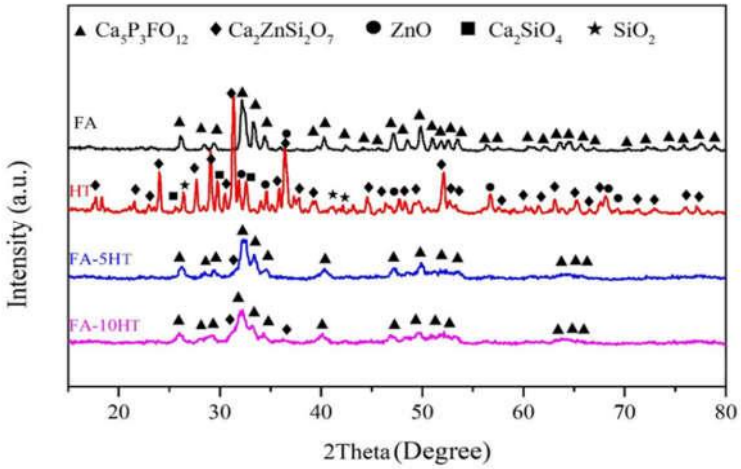

Figure 5. X-ray diffraction patterns of FA powder, HT powder, and FA-HT scaffolds with various HT concentrations (a) FA, (b) HT, (c) FA-5HT and (d) FA-10HT

3.2. Compressive strength

Fig. 6 shows the compressive stress–strain curves for fluorapatite scaffolds containing different percentages of hardystonite. Three different zones are observable in the stress-strain curve of both samples. According to previous studies about porous ceramic scaffolds synthesized by space holder method, these zones are described as follow: Zone 1: a linear zone with a direct relationship between stress and strain, and Young's module can be calculated using the slope of this line. This zone finishes at the maximum compression strength. Zone 2: indicates breaking apart of pores under pressure. Zone 2: shows the densification of scaffolds and closure of pores as the pressure increases [28]. Bone scaffolds should possess a compressive strength similar to that of the neighboring bones.

As it is shown in Fig. 6, the compressive strength of scaffolds increases as the amount of hardystonite increased. The maximum compressive strength for FA-5HT scaffolds was about 1.6 MPa, while this value was about 2.8 MPa for FA-10HT scaffold. The calculated Young's modulus value for these scaffolds was 5.5 MPa and 12.4 MPa, respectively. Actually, FA powder acts as reinforcement phase and fluxes in the composite scaffold which leads to decline of the sintering temperature and eventually an enhancement in mechanical properties [28]. The area under the curve is the other important point, which shows toughness and ductility of samples and increases by increasing the hardystonite amount. It shows that addition of hardystonite decreased brittleness of fluorapatite. These results match with the result of previous studies. For example, Guidar et al. [28] showed that fluorapatite alone has very low strength and cannot be used in bone tissue engineering; so they increased its mechanical properties by adding alumina to the fluorapatite matrix and made it able to bear mechanical loading. Some other studies showed [29] that it is possible to composite fluorapatite with polymers in order to improve its toughness. For example Guo et al. [29] had synthesized scaffolds with optimal mechanical properties for tissue engineering by compositing fluorapatite with polycaprolactone (PCL).

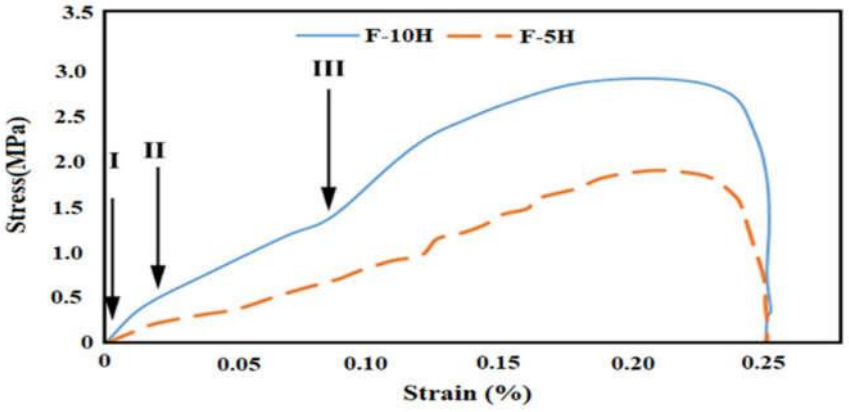

Figure 6. Compressive stress-strain diagram of samples

Previous studies showed that compressive strength of dense bone (cortical bone) ranges from 130 to 180 MPa, and that of spongy bone ranges from 0.2 to 4 MPa. Compressive strength of present scaffold was about 1.6-2.8 MPa which falls exactly in the range of porous bone compressive strength. So it can be claimed that the synthesized scaffolds in this study have the potential to be used in bone tissue engineering.

3.3. Apatite formation ability

Samples were immersed in SBF solution for 28 days in order to study the Apatite-forming ability of FA-HT scaffolds [26]. SEM micrographs show the surface of Mon and FA-HT scaffolds after incubation in SBF for 28 d along with corresponding EDS analysis (Fig. 7).

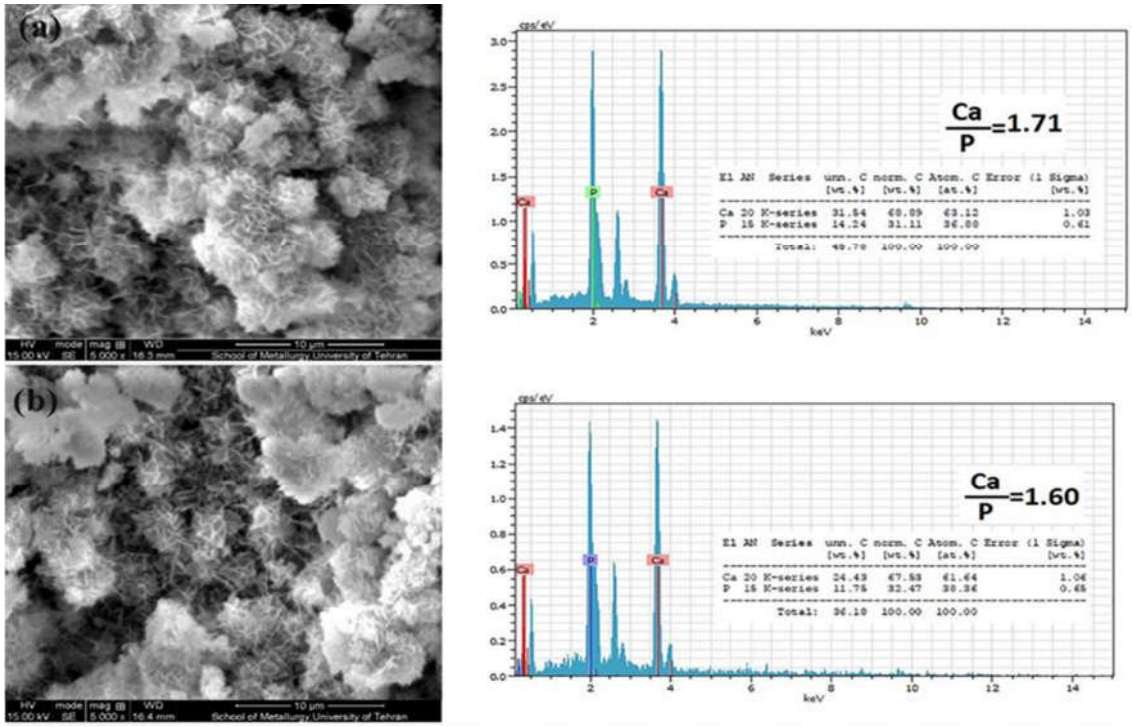

Figure 7. SEM images and EDS results of a) F-5H and b) F-10H samples after 21 days of immersion in SBF

As can be seen, the formation of a dense apatite layer on the surface of all scaffolds. The EDS analysis confirmed the presence of calcium and phosphorus elements in these compounds. The results of calcium to phosphorous (Ca/P) ratio measurements formed on the surface of the FA-5HT and FA-10HT scaffolds which were calculated by EDS analysis, showed values of 1.71 and 1.60, respectively. These values are almost close to the Ca/P ratio in hydroxyapatite composition. The results of the EDS analysis indicated a lower Ca/P ratio in FA-10HT scaffold than that of the FA-5HT sample. Based on previous studies, there is not a positive correlation between higher values of Ca/P ratio and higher ability in apatite-formation. Diba et al. [1] compared the apatite-forming ability of calcium-silicate compositions and reported that among all compositions, hardystonite has the lowest apatite-forming ability and a lower degradation rate, due to its high chemical stability. Some studies showed that the existence of Ca and Zn elements in hardystonite delay the apatite's nucleation. Hardystonite is known to be a bioactive ceramic. Apatite nucleation mechanisms on hardystonite surface are related to releasing of calcium, zinc, and silicon ions of SBF solution. In the first days of release, these ions increase the pH value of the solution and alkalize it. Ca^{2+} ions in hardystonite can be replaced by the existing H^{+} ions in the solution and causes the formation of silane (Si-OH) groups on the surface of hardystonite. This hydrated layer is a desirable place for apatite nucleation. As time passes, apatite adds OH^{-} ions to the solution and reduces its pH [18,31]. Previous studies showed that apatite nucleation mechanism in fluorapatite is related to Ca^{2+} and PO_4^{3-} ions in the solution. These ions increase the saturation degree of the solution and create a favorable environment for calcium-phosphate nucleation over time. It is noteworthy that as the immersion time increase, dissolution rate of apatite increases too and boosts the apatite nucleation; so a dense layer of apatite covers the whole surface of samples [32].

4. CONCLUSION

In the present study, the fluorapatite-hardystonite (FA-HT) nanocomposite scaffolds with different amount of HT (5 and 10% wt.) were fabricated via the space holder method. The XRD results of the synthesized scaffolds confirmed the formation of FA and HT powders. The FA-HT nanocomposite scaffolds possessed a high level of porosity (81–83%) with pore size in the range of 400–600 μm. The scaffolds had an interconnected network which makes them appropriate for bone tissue engineering. The results also revealed that mechanical property of scaffolds increased by increasing the HT content; the compressive strength values of FA-5HT and FA-HT scaffolds were measured 1.6 MPa and 2.8 MPa, respectively. The Young modulus value for these scaffolds was 5.5 MPa and 12.4 MPa, respectively. Based on the results of bioactivity test, the Ca/P ratio of FA-5HT and FA-10HT samples was 1.71±0.3 and 1.60±0.5, respectively which implying high apatite formation ability of the samples.

REFERENCES

1. Diba, M., Goudouri, O.-M., Tapia, F., Boccaccini, A.R., "Magnesium-containing bioactive polycrystalline silicate-based ceramics and glass-ceramics for biomedical applications", ***Current opinion in solid state and materials science***, Vol. 18, No. 3, (2014),147-167.
2. Bakhsheshi-Rad, H.R., Hamzah, E., Daroonparvar, M., Ebrahimi-Kahrizsangi, R., Medraj, M., "In-vitro corrosion inhibition mechanism of fluorine-doped hydroxyapatite and brushite coated Mg–Ca alloys for biomedical applications", ***Ceramics International***, Vol. 40, No. 6, (2014), 7971-7982.
3. Bakhsheshi-Rad, H.R., Chen, X.B., Ismail, A.F., Aziz, M., Hamzah, E., Najafinezhad, A., "A new multifunctional monticellite-ciprofloxacin scaffold: Preparation, bioactivity, biocompatibility, and antibacterial properties", ***Materials Chemistry Physics***, Vol. 222, (2019), 118-131.
4. Chen, X., Ou, J., Kang, Y., Huang, Z., Zhu, H., Yin, G., Wen, H., "Synthesis and characteristics of monticellite bioactive ceramic", ***Journal of Matrials Science***, Vol. 19, No. 3, (2008), 1257–63.
5. Lipskas, J., Deep, K., Yao, W., "Robotic-assisted 3D bio-printing for repairing bone and cartilage defects through a minimally invasive approach", ***Scientific Reports***, Vol. 9, No. 1, (2019), 3746.
6. Bakhsheshi-Rad, H.R., Hamzah, E., Abbasizadeh, N., Najafinezhad, A., Kashefian, M., "Synthesis of novel nanostructured bredigite–amoxicillin scaffolds for bone defect treatment: cytocompatibility and antibacterial activity", ***Journal of Sol-Gel Science and Technology***, Vol. 86, No. 1, (2018), 83–93.
7. Khanna, K., Jaiswal, A., Dhumal, R. V., Selkar, N., Chaudhari, P., Soni, V.P., Vanage, G.R., Bellare, J., "Comparative bone regeneration study of hardystonite and hydroxyapatite as filler in critical-sized defect of rat calvaria, ***RSC Advances***, Vol. 7, No. 60, (2017), 37522–33.
8. Akogo, D.A., Palmer, X.-L., "ScaffoldNet: Detecting and classifying biomedical polymer-based scaffolds via a convolutional neural network", In: Arai K., Bhatia R. (eds) Advances in Information and Communication. FICC 2019. Lecture Notes in Networks and Systems, Vol. 70, (2020), 152–61.
9. Bakhsheshi-Rad, H.R., Hamzah, E., Daroonparvar, M., Saud, S.N., Abdul-kadir, M.R., "Bi-layer nano-TiO_2/FHA composite coatings on Mg–Zn–Ce alloy prepared by combined physical vapour deposition and electrochemical deposition methods", ***Vacuum***, Vol. 110, (2014), 127-135.
10. Bakhsheshi-Rad, H.R., Hamzah, E., Staiger, M.P., Dias, G.J., Hadisi, Z., Saheban, M., Kashefian, M., "Drug release, cytocompatibility, bioactivity, and antibacterial activity of doxycycline loaded Mg-Ca-TiO_2 composite scaffold", ***Materials & Design***, Vol. 139, (2018), 212–21.
11. Hadisi, Z., Nourmohammadi, J., Nassiri, S.M., "The antibacterial and anti-inflammatory investigation of Lawsonia Inermis-gelatin-starch nano-fibrous dressing in burn wound", ***International journal of biological macromolecules***, Vol. 107, (2018), 2008-2019.
12. Shao, H., He, J., Lin, T., Zhang, Z., Zhang, Y., Liu, S., "3D gel-printing of hydroxyapatite scaffold for bone tissue engineering", ***Ceramics International***, Vol. 45, No. 1, (2019), 1163–70.
13. Bakhsheshi-Rad, H.R., Hamzah, E., Ismail, A.F., Aziz, M., Hadisi, Z., Kashefian, M., Najafinezhad, A., "Novel nanostructured baghdadite-vancomycin scaffolds: In-vitro drug release, antibacterial activity and biocompatibility", ***Materials Letters***, Vol. 209, (2017), 369-372.
14. Algarni, H., AlShahrani, I., Ibrahim, E.H., Eid, R.A., Kilany, M., Ghramh, H.A., Shaaban, E.R., Reben, M., "Nano and microstructure of bioglasses: In vitro and in vivo bioactivity properties", ***Journal of Non-Crystalline Solids***, Vol. 512, (2019),

72–80.
15. Caballero, S.S.R., Elsayed, H., Tadier, S., Montembault, A., Maire, E., David, L., Delair, T., Colombo, P., Grémillard, L., "Fabrication and characterization of hardystonite-chitosan biocomposite scaffolds", ***Ceramics International,*** Vol. 45, No. 7, (2019), 8804-8814.
16. Tavangar, B., Arasteh, S., Edalatkhah, H., Salimi, A., Doostmohammadi, A., Seyedjafari, E., "Hardystonite-Coated Poly(l-lactide) Nanofibrous Scaffold and Efficient Osteogenic Differentiation of Adipose-Derived Mesenchymal Stem Cells", ***Artificial Organs,*** Vol. 42, No. 11, (2018), E335-E348.
17. Singh, S., Vashisth, P., Shrivastav, A., Bhatnagar, N., "Synthesis and characterization of a novel open cellular Mg-based scaffold for tissue engineering application", ***Journal of the mechanical behavior of biomedical materials***, Vol. 94, (2019), 54–62.
18. Bakhsheshi-Rad, H.R., Hamzah, E., Ismail, A.F., Aziz, M., Najafinezhad, A., Daroonparvar, M., "Synthesis and in-vitro performance of nanostructured monticellite coating on magnesium alloy for biomedical applications", ***Journal of Alloys and Compounds,*** Vol. 773, (2019), 180-193.
19. Bartoš, M., Suchý, T., Foltán, R., "Note on the use of different approaches to determine the pore sizes of tissue engineering scaffolds: what do we measure?", ***Biomedical Engineering Online,*** Vol. 17, No. 1, (2018), 110.
20. Porter, J.R., Ruckh, T.T., Popat, K.C., "Bone tissue engineering: a review in bone biomimetics and drug delivery strategies", ***Biotechnology Progress,*** Vol. 25, No. 6, (2009), 1539–1560.
21. Dayaghi, E., Bakhsheshi-Rad, H.R., Hamzah, E., Farid, A., Ismail, A.F., Aziz, M., Abdolahi, E., "Magnesium-zinc scaffold loaded with tetracycline for tissue engineering application: In vitro cell biology and antibacterial activity assessment", ***Materials Science and Engineering: C,*** Vol. 102, (2019), 53–65.
22. Gomes, M., Reis, R., "Tissue engineering: key elements and some trends", ***Macromolecular bioscience***, 4(8), (2014), 737-742.
23. Wang, B., Konstantinov, K., Wexler, D., Liu, H., Wang, G., "Synthesis of nanosized vanadium pentoxide/carbon composites by spray pyrolysis for electrochemical capacitor application", ***Electrochimica Acta***, Vol. 54, No. 5, (2009), 1420-1425.
24. Kumar, J.P., Lakshmi, L., Jyothsna, V., Balaji, D.R., Saravanan, S., Moorthi, A., Selvamurugan, N., "Synthesis and characterization of diopside particles and their suitability along with chitosan matrix for bone tissue engineering in vitro and in vivo", ***Journal of biomedical nanotechnology***, Vol. 10, No. 6, (2014), 970–81.
25. Choudhary, R., Koppala, S., Swamiappan, S., "Bioactivity studies of calcium magnesium silicate prepared from eggshell waste by sol-gel combustion synthesis", ***Journal of Asian Ceramic Societies***, Vol. 3, No. 2, (2015), 173–7.
26. Kokubo, T., Ito, S., Huang, Z.T., Hayashi, T., Sakka, S., Kitsugi, T., Yamamuro, T., "Ca, P□rich layer formed on high□strength bioactive glass□ceramic A□W.", ***Journal of biomedical materials research***, Vol. 24, No. 3, (1990), 331–43.
27. Saheban, M., Bakhsheshi-Rad, H.R., Kasiri-Asgarani, M., Hamzah, E., Ismail, A.F., Aziz, M., Dayaghi, E., "Effect of zeolite on the corrosion behavior, biocompatibility and antibacterial activity of porous magnesium/zeolite composite scaffolds", ***Materials Technology***, Vol. 34, No. 3, (2019), 258-269.
28. Ghorbel, H.F., Guidara, A., Danlos, Y., Bouaziz, J., Coddet, C., "Synthesis and characterization of alumina-fluorapatite coatings deposited by atmospheric plasma spraying", ***Materials Letters***, Vol. 185, (2016), 268-271.
29. Guo, T., Li, Y., Cao, G., Zhang, Z., Chang, S., Czajka-Jakubowska, A., et al. Fluorapatite-modified scaffold on dental pulp stem cell mineralization. ***J Dent Res,*** Vol. 93, (2014), 1290–5.
30. Bakhsheshi-Rad H.R., Hamzah E., Ismail A.F., Nör, J.E., Clarkson, B.H., Liu, J., "Novel bi-layered nanostructured SiO_2/Ag-FHAp coating on biodegradable magnesium alloy for biomedical applications", ***Ceramics International***, Vol. 42, No. 10, (2016), 11941-11950.
31. Kheradmandfard, M., Fathi, M.H., Ansari, F., Ahmadi, T., "Effect of Mg content on the bioactivity and biocompatibility of Mg-substituted fluorapatite nanopowders fabricated via mechanical activation", ***Materials Science and Engineering: C***, Vol. 68, (2016), 136–42.
32. Choudhary, R., Chatterjee, A., Venkatraman, S.K., Koppala, S., Abraham, J., Swamiappan, S., "Antibacterial forsterite (Mg_2SiO_4) scaffold: A promising bioceramic for load bearing applications", ***Bioactive Materials,*** Vol. 3, No. 3, (2018), 218-224.